Physica A 432 (2015) 301–314

Contents lists available at ScienceDirect

Physica A

journal homepage: www.elsevier.com/locate/physa

Volatility behavior of visibility graph EMD financial time series from Ising interacting system

Bo Zhang [a], Jun Wang [a], Wen Fang [b,*]

[a] Department of Mathematics, School of Science, Beijing Jiaotong University, Beijing 100044, PR China
[b] Department of Finance, School of Economics and Management, Beijing Jiaotong University, Beijing 100044, PR China

HIGHLIGHTS

- A financial price model is developed and investigated by stochastic Ising system.
- Empirical mode decomposition is used to decompose financial data into different frequency series.
- Volatility behavior of returns for financial time series is studied by visibility graph and horizontal visibility graph.
- Complexity analysis is performed for the considered series.
- Statistical analysis illustrates that the simulation data could exhibit the similar properties as the real data.

ARTICLE INFO

Article history:
Received 25 December 2014
Received in revised form 1 March 2015
Available online 30 March 2015

Keywords:
Financial time series model
Stochastic Ising system
Empirical mode decomposition
Volatility analysis
Visibility graph
Horizontal visibility graph

ABSTRACT

A financial market dynamics model is developed and investigated by stochastic Ising system, where the Ising model is the most popular ferromagnetic model in statistical physics systems. Applying two graph based analysis and multiscale entropy method, we investigate and compare the statistical volatility behavior of return time series and the corresponding IMF series derived from the empirical mode decomposition (EMD) method. And the real stock market indices are considered to be comparatively studied with the simulation data of the proposed model. Further, we find that the degree distribution of visibility graph for the simulation series has the power law tails, and the assortative network exhibits the mixing pattern property. All these features are in agreement with the real market data, the research confirms that the financial model established by the Ising system is reasonable.

1. Introduction

Financial market is a complex evolving dynamic system, consisting of a large number of agents (investors) interacting with one another in complicated ways, which reacts to external investment information to determine the best price for a given asset. Nowadays, the analysis of financial systems based on stochastic dynamics has become one the of active-research topics in financial research. As the stock markets are becoming deregulated worldwide, the modeling of dynamics of forward prices is becoming a key problem in the risk management, physical assets valuation, derivatives pricing and so on, see Refs. [1–26]. Meanwhile, the opinion that the price fluctuations are due to the interactions among the market investors is being widely accepted. For the financial modeling, aiming to understand price fluctuations, in an attempt to reproduce the stochastic behaviors of financial time series, any model needs to define a mechanism for the formation of the price. And the

* Corresponding author. Tel.: +86 1051684612.
E-mail address: fangwen@bjtu.edu.cn (W. Fang).

http://dx.doi.org/10.1016/j.physa.2015.03.057
0378-4371/

behaviors of price changes in financial markets have long been a focus of economic research for a more clear understanding of mechanism and characteristics of financial markets. A complex behavior can emerge due to the interactions among smallest components of that system [27], and it is also a successful strategy to analyze the behavior of a complex system by studying these components. In the empirical research, some statistical properties for market fluctuations are revealed by high frequency financial time series, for instance, fat-tail phenomenon, power-law distribution and volatility clustering and so on [7,16,28–30]. Further, a volatility forecast and a second prediction on the volatility of volatility over the defined period is needed to price derivative contracts. Early models of volatility measurement include the work of Engle [31]. Engle developed a class of models known as autoregressive conditional heteroskedasticity (ARCH). Bollerslev [32] extended the ARCH to include past variance in the conditional variance function and this extension is widely known as the GARCH model. These models have gained popularity because they are capable of capturing volatility clustering and can accommodate fat-tailedness of return distribution at the same rate of persistence [33,34].

Recently, some researchers apply statistical physics systems (or interacting particle systems) to measure and explain this set of empirical facts. On one hand, economic systems such as financial markets are similar to physical systems in that they are comprised of a large number of interacting "agents". On the other hand, they are quite different and much more complex because economic agents are "thinking" units and they interact in complicated ways not yet quantified. Indeed, most physics approaches to finance view financial markets as a complex evolving system [35]. For example, Stauffer and Penna [11] applied the lattice percolation theory to the market fluctuations, and their model was based on the herding effect by which traders follow trends without considering any economic data. The existence of heavy tail behavior for the returns was found when the influence rate of the model is around or at a critical value. Krawiecki [10] and Fang and Wang [4,5] developed an interacting-agent model of speculative activity explaining price formation in financial market that is based on the stochastic Ising dynamic system. Lux and Marchesi [14] introduced an agent-based model in which chartist agents compete with fundamentalists agents, leading to power law distributed returns as observed in real markets which contradicts the popular efficient market hypothesis.

In the present work, we make an approach to establish a price model through the stochastic Ising system. In the proposed model, all of spins are flipped by following Ising dynamic system. We suppose that traders determine their positions at each time by observing and diffusing the market information, each trader is thought to be a subunit in the stock market, and may take positive (buying) position or negative (selling) position, denoted by $+$ and $-$ separately. We use Ising dynamic system to investigate the fluctuation of the stock market because that system consists of subunits. In this work, applying two kinds of graph based time series analysis methods, visibility graph [36,37] and horizontal visibility graph [38], we study the statistical behaviors of absolute return series and their corresponding IMFs (figured out by the empirical mode decomposition (EMD) method, which is used to decompose the data into a few lower frequency series [39,40]), and present some empirical relationship between the topological characteristic and the original time series. Furthermore, the complex properties of original return series and IMFs series after EMD are investigated by multiscale entropy analysis (MSE). It is a method to measure the disorder and complexity at multiple time scales [41,42]. To verify the feasibility of the proposed model, the simulation data and the real stock data of Shanghai Composite Index (SSE) and Hang Seng Index (HSI) are compared.

2. Financial time series model derived from Ising system

2.1. Brief description of Ising system

Ising dynamic system is one of stochastic interacting particle systems [43–48]. Let $\mathbb{Z}^2$ be the usual $2D$ square lattice and we denote by $\mathfrak{B}$ the set of bonds of the lattice (pairs of nearest neighbors). Let $\Omega_{\mathbb{Z}^2} = \{+1, -1\}^{\mathbb{Z}^2}$ denote the space of spin configurations on $\mathbb{Z}^2$, an element of $\Omega_{\mathbb{Z}^2}$ usually denote by $\sigma = \{\sigma_i : i \in \mathbb{Z}^2\}$. The spin σ_i take one of the integer values $+1$ or -1. We consider the Ising model with the following dynamic system of Hamiltonian, for every $\sigma \in \Omega$

$$H_{\mathbb{Z}^2,b}(\sigma) = -J \sum_{\langle i,j\rangle} \delta_{\sigma_i,\sigma_j} - b \sum_i \delta_{\sigma_{i,1}} \tag{1}$$

where $J > 0$ for the ferromagnetic systems and δ is the Kroeneker symbol. The first sum is over all nearest neighbors (denote by $\langle i, j\rangle$) on the lattice and the second sum over all lattice points. Here the applied magnetic field b acts on the (arbitrarily chosen) state 1. Then the partition function is

$$Z_{\mathbb{Z}^2,h}(\sigma) = \sum_\sigma \exp\left(K \sum_{\langle i,j\rangle} \delta_{\sigma_i,\sigma_j} + h \sum_i \delta_{\sigma_{i,1}}\right) \tag{2}$$

where $K = \beta J$ and $h = \beta b$, $\beta = 1/(k_B T)$, k_B and T being Boltzmann's constant and temperature, respectively.

The spins in Ising model can point up (spin value $+1$) or point down (spin value -1), and the grain flips between the two orientations. As β approaches the critical inverse temperature β_c from below, spin fluctuations are present at all scales of length. When $\beta = \beta_c$, the correlations decay by a power law, while for $\beta > \beta_c$, there exist two distinct pure phases, i.e., the Ising model exhibits the phase transition, for more details see Refs. [43–45]. Correlations play a significant role in studying the fluctuations of the phase interfaces for the statistical physics model, see Refs. [44,48]. In the following of present work,

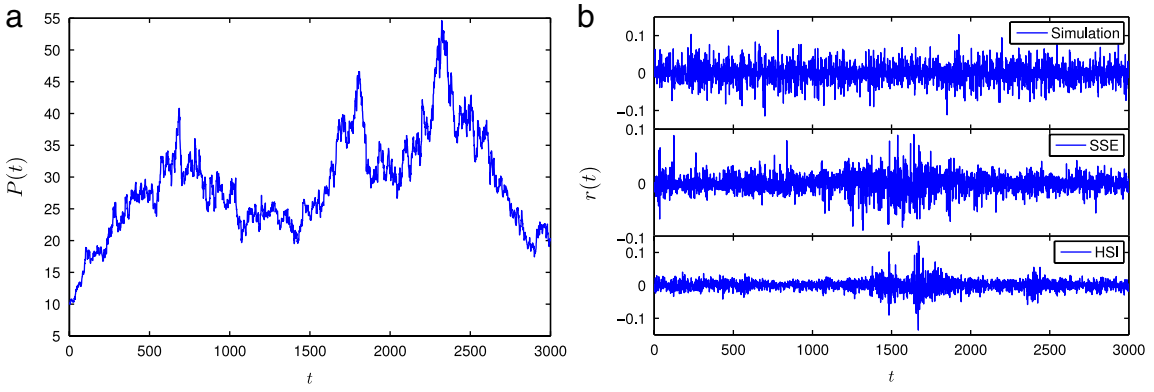

Fig. 1. (a): Fluctuations of the simulation prices when $\beta = 0.8$. (b): (From the top figure to the bottom one): The corresponding simulation returns of (a), SSE returns, HSI returns.

we consider the Ising model with the zero external magnetic field ($b = 0$ and $h = 0$). Under this condition, we only focus on the interaction between spins in the lattice $\mathbb{Z}^2$. Market information is spreading by agents, therefore we main consider the interaction between investors.

2.2. Financial price time series model

In this section, the Ising model is employed to model and reproduce the financial time series. Ising model is composed of numerous interacting spins, which have similarity with financial markets consisting of a large number of interacting investors [43–45]. The fluctuation of stock prices is attributed to the information flowing in the financial market, which is according with the interaction among the spins in an Ising system. Consider a model of auctions for a stock in a stock market, we derive the stock price process from the auctions. We assume that 2D-lattice Ising model has L^2 spins, every spin in the lattice is regarded as a trader, so there are L^2 traders in the proposed stock market. Suppose that each trader can trade one unit number of stocks at each time $t \in \{1, 2, \ldots, T\}$. At each time t, the fluctuation of stock price process is especially influenced by the number of traders $m^+(t)$ who take buying positions and the number of traders $m^-(t)$ who take selling positions. If the number of traders in selling positions is smaller than that of traders in buying positions, it implies that the stock price is considered to be low by the market participants, and the stock auctions higher searching for buyers, similarly for the opposite case. In the 2D-lattice we define each point as $m_{ij}(t)$ which also considered as investing position ($1 \le i \le L$, $1 \le j \le L$) at time t. And let $m(t) = (m_{11}(t), \ldots, m_{1L}(t), \ldots, m_{L1}(t), \ldots, m_{LL}(t))$ be the configuration of positions for L^2 traders. The space of all configurations of positions for L^2 traders from time 1 to t is defined by $\mathcal{M} = \{m = (m(1), \ldots, m(t))\}$. For a given configuration $m \in \mathcal{M}$ and a trading time t, let $m^-(t)$ denote the number of corresponding minus spins (the number of traders with taking selling positions), and let $m^+(t)$ denote the number of corresponding plus spins (the number of traders with taking buying positions). Then we define

$$\mathscr{D}(t) = m^+(t) - m^-(t). \tag{3}$$

If $\mathscr{D}(t) > 0$, there are more buyers than sellers, then the stock price is auctioned up, similarly for the opposite case. From the above description and [12,49], the stock price of the model at time t ($t = 1, 2, \ldots, T$) is defined as

$$\mathscr{P}_t = \mathrm{e}^{\gamma \mathscr{D}(t)/L^2} \mathscr{P}_{t-1}, \qquad \mathscr{P}_t = \mathscr{P}_0 \exp\Big\{\gamma \sum_{k=1}^{t} \frac{\mathscr{D}(k)}{L^2}\Big\} \tag{4}$$

where $\mathscr{P}_0$ represents the initial stock price, $\gamma > 0$ is the depth parameter of the market which measures sensitivity of price fluctuation in response to change in excess demand. For receiving a desired simulation, γ is set to be a random variable obeying uniform distribution in [0, 1]. The formula of single-period stock logarithmic returns from $t - 1$ to t is given by

$$r(t) = r_t = \ln \mathscr{P}_t - \ln \mathscr{P}_{t-1}, \quad t = 1, 2, \ldots, T. \tag{5}$$

In this paper, we analyze the logarithmic returns for the daily price changes. And the volatility $v(t)$ of time series, defined for simplicity as the absolute returns $v(t) = |r(t)|$ [10]. Depending on the price model by Ising system with parameters $\beta = 0.8$ and $L = 100$, the fluctuations of stock prices and the corresponding returns is exhibited in Fig. 1.

3. Methodologies of statistical analysis

3.1. Empirical mode decomposition algorithm

Empirical mode decomposition (EMD) is an innovative data processing algorithm for nonlinear and nonstationary time series [39,40,50,51]. The main idea of EMD is to locally decompose any time series into a sum of a local detail and a local

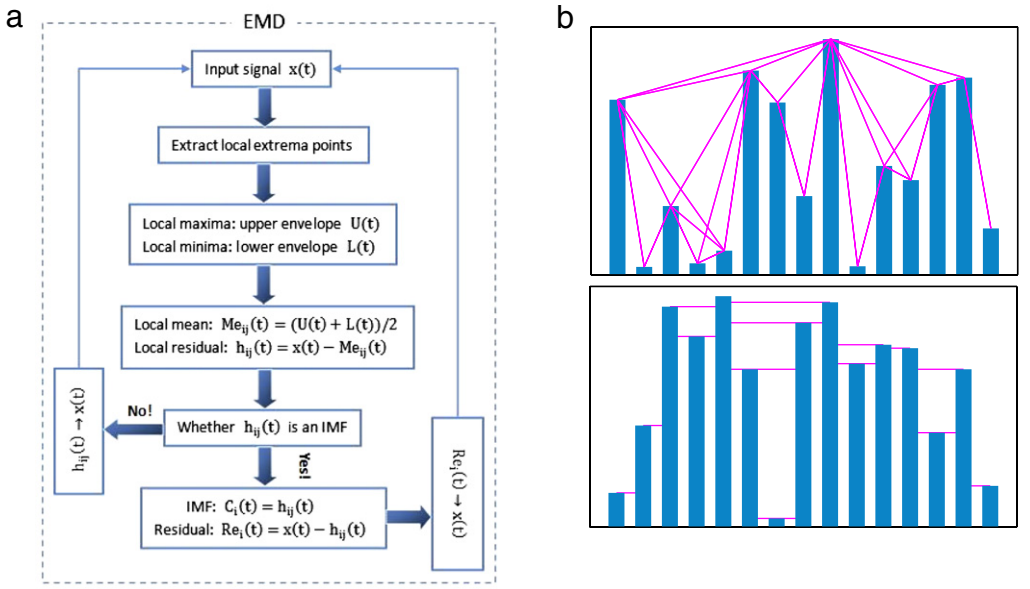

Fig. 2. (a) A flowchart of the empirical mode decomposition. (b) Top: Plot of visibility graph algorithm; Bottom: Plot of horizontal visibility graph algorithm.

trend, correspondingly, for a high frequency part and a low frequency part. The latter is called the residual and the former is called the intrinsic mode functions (IMFs), which represent the different scales of the original time series and form the adaptive and physical basis of the data. The EMD will reduce the data (which represent $r(t)$ in this paper) into a collection of IMF defined as any function satisfying the following conditions: (a) in the whole data set, the number of extrema and the number of zero-crossings must either equal or differ at most by one; (b) at any point, the mean value of the "upper envelope" (defined by the local maxima) and the "lower envelope" (defined by the local minima) is zero. Actually, the EMD is a sifting process, which can be described with six steps, we illustrate the EMD algorithm in Fig. 2(a). In this figure, Re_n is a residual which is generally a constant or a monotonic function representing the trend of the time series.

3.2. Graph theory: visibility graph and horizontal visibility graph

Visibility graph (VG). Complex network theory is a new branch of statistical physics, it describes complex system with networks [52,53]. The visibility graph algorithm maps a time series into a network and the constructed graph inherits several properties of the series in its structure [22,36,37]. A study of the network may reveal some interesting and useful information of the time series. The VG method was mainly applied to investigate the dynamical properties of continuous signals [54], was applied also to point processes (sequence of events randomly occurring in time) [55,56] or other field [57–59]. The visibility algorithm transforms a time series $\{x_i\}_{i=1,\ldots,N}$ into a visibility graph $G = \langle V, E\rangle$, where $V = \{v_i\}_{i=1,\ldots,N}$ is the set of vertex with the vertex v_i corresponding to the data point x_i. E is the edge of the graph. Then we define $A = \{a_{i,j}\}_{i,j=1,\ldots,N}$ as the adjacent matrix of the visibility graph with $a_{i,j} = 1$ for connected vertices and $a_{i,j} = 0$ for disconnected ones. The element $a_{i,j} = 1$ when the following geometrical criterion is fulfilled:

$$\frac{x_i - x_k}{i - k} > \frac{x_i - x_j}{i - j}, \quad i < k < j \tag{6}$$

where x_k is any other data points between x_i and x_j. Otherwise, $a_{i,j} = 0$. Absolutely, if the above equation is established, we call the two nodes v_i and v_j are connected and the corresponding data points x_i and x_j are visible to each other. Thus an unweighted network VG can be constructed based on a time series. For illustration, we plot the construction of visibility graph for a random time series of length 15 in Fig. 2(b).

Horizontal visibility graph (HVG). The horizontal visibility algorithm is a variant of the visibility algorithm, which is essentially similar to the former with a geometrically simpler visibility criterion [37]. HVGs realize a methodology in the analysis of time series, their degree distribution being a good discriminator between randomness and chaos [38]. The horizontal visibility algorithm transforms a time series $\{x_i\}_{i=1,\ldots,N}$ into a horizontal visibility graph. The difference from the former algorithm is its adjacent matrix, whose element $a_{i,j} = 1$ if every point x_k between x_i and x_j fulfill the following condition:

$$x_i, x_j > x_k, \quad i < k < j. \tag{7}$$

Otherwise, $a_{i,j} = 0$, meaning that the data point x_i is not horizontally visible to the data x_j and meanwhile the corresponding vertices v_i and v_j are not connected. For illustration, we plot the construction of horizontal visibility graph for a random time series of length 15 in Fig. 2(b).

Table 1
Descriptive statistical properties of returns for HSI, SSE and the price model.

β	Min	Max	Mean	St. D.	Kurtosis	Skewness
0.7	−0.0869	0.0861	3.45E−05	0.0134	8.9696	−0.0414
0.8	−0.0980	0.1101	−3.42E−04	0.0176	7.3672	−0.1798
0.9	−0.1435	0.1190	1.61E−04	0.0229	6.7246	0.0054
HSI	−0.1358	0.1341	2.23E−04	0.0153	12.3398	0.0511
SSE	−0.0862	0.0903	1.33E−04	0.0162	6.7277	−0.1283

Note: St. D. represents standard deviation.

Vertex degree distribution. Vertex degree distribution is one of the most important characteristics of complex networks [22,60]. The degree of a vertex in a network is the number of connections it has to other nodes, it is equal to the number of edges connected to that vertex. Here we define p_k to be the fraction of vertices in the network having degree k, or the probability that a vertex chose uniformly at random has degree k. Thus the complementary cumulative distribution function can be presented as follows

$$P(k) = \sum_{i=k}^{\infty} p(i). \tag{8}$$

That is the probability that the degree is greater than or equal to k. Then we may have the plot of $P(k)$ vs. k.

Assortative mixing pattern. In most kinds of networks there are at least a few different types of vertices, and the probability of connection between vertices often depends on types. This kind of selective linking is called assortative mixing or homophily and has been widely studied [60]. Mixing pattern is an important statistical characteristic of complex networks [60–62]. Assortative mixing refers to the phenomenon that nodes in a networks are more likely connected to nodes that are alike them in some way.

The mixing pattern can be measured by the Pearson coefficient

$$\sigma = \frac{N_e^{-1}\sum_i j_i h_i - \left[N_e^{-1}\sum_i \frac{1}{2}(j_i + h_i)\right]^2}{N_e^{-1}\sum_i \frac{1}{2}(j_i^2 + h_i^2) - \left[N_e^{-1}\sum_i \frac{1}{2}(j_i + h_i)\right]^2} \tag{9}$$

where N_e is the edges' total number, j_i and h_i denote the degrees of the two vertices at the ends of edge i. If $\sigma > 0$, the network is assortative. Otherwise, the network is disassortative.

A special case of assortative mixing according to a scalar vertex property is mixing according to vertex degree, also commonly referred to simply as degree correlation. In this case, we want to determine whether the high-degree vertices associate preferentially with other high-degree vertices. The case of assortative mixing by degree topology, degree correlation can give rise to some interesting network structure effects. For a given network, the average degree $\langle k_n \rangle$ of the nearest neighbors of nodes having degree k is determined, k_n represents the degree of vertex n. If $\langle k_n \rangle$ increases with k, high-degree vertices associate preferentially with other high-degree vertices and the network is assortative.

4. Empirical analysis of actual and simulation data

4.1. Data set

In the following parts, we intend to detect some statistical behaviors of the simulation data derived from the random price model based on the Ising system and the real market indices in comparison. In the Ising system, the critical temperature parameter $\beta_c \approx 0.88$ [26]. Nearby β_c, the drastic phase transition of spins is very similar to the rapid information spreading in the financial market. In addition, Stauffer and Penna developed a financial time series model by lattice percolation, where the critical phenomenon of percolation is used to illustrate the herd behavior of stock market participants [11] In that price model, we fixed the length $L = 100$, so the number of traders is 10^4, then we set the temperature parameter β to be 0.7, 0.8 and 0.9 and choose three corresponding time series, each covering 3000 data points respectively. For the real data, we choose the Shanghai Composite Index and the Hang Seng Index both from Jan 21, 2002 to Mar 17, 2014 separately with 2940 data points and 3000 data points.

4.2. Descriptive statistical analysis of returns for the price model

After the data is obtained, we first want to test whether our simulation data is able to capture the well-known dynamic statistical properties that are uncovered in the financial markets [6,19]. So we calculate kurtosis and skewness in Table 1. It is known that the kurtosis shows the centrality of data and the skewness shows the symmetry of data, the kurtosis and

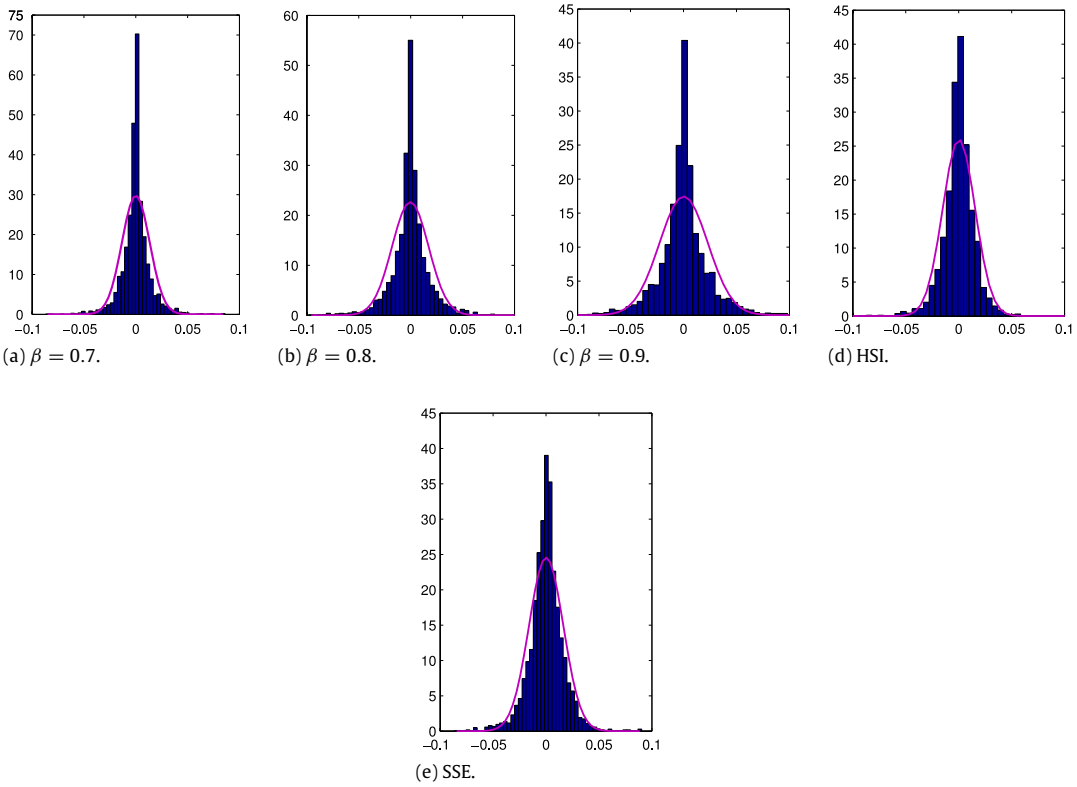

(a) $\beta = 0.7$. (b) $\beta = 0.8$. (c) $\beta = 0.9$. (d) HSI.

(e) SSE.

Fig. 3. Histograms of returns for simulation series and real indices. The curve in each figure is the corresponding normal fitting curve.

Table 2
Jarque Bera test of returns for parameter β, SSE and HSI.

β	Capacity	JB statistic	Critical value	H	p-value
0.7	3000	4.46E+03	5.9704	1	0.001
0.8	3000	2.40E+03	5.9704	1	0.001
0.9	3000	1.73E+03	5.9704	1	0.001
HSI	3000	1.09E+04	5.9704	1	0.001
SSE	2940	1.71E+03	5.9701	1	0.001

the skewness of Gaussian distribution are respective 3 and 0. We find that the kurtosis value (which are all higher than 3) decreases with the increasing of β, and skewness all deviated from 0, thus the fat-tail is visible compared to the Gaussian distribution. And the histograms of returns for each series is shown in Fig. 3. That means our simulation data is deviated from Gaussian distribution, the property is conformed to the real market data.

For further analyzing the statistical character of returns distributions for SSE, HSI and simulation data, we make the Jarque Bera test by the statistical method and filled in Table 2. The null hypothesis is that the data vector obeys the standard normal distribution ($H = 0$), the alternative hypothesis is that the sample does not have the distribution ($H = 1$). If the test statistic is larger than the critical value, that means the null hypothesis can be rejected at a significance level of 5%. Each value of H is 1 in Table 2, easily, we can clearly clarify that all the time series including simulation data and real data does not follow Gaussian distribution.

4.3. Data decomposition by EMD method

As introduced in Section 3.1, we aim to process data with EMD method to achieve their corresponding IMFs series. Then the statistical behaviors of IMFs and the original series will be studied. We take logarithmic return r_t of SSE, HSI and the simulation data as the primary time series, and then apply EMD to decompose r_t into 10 IMFs and their residuals respectively. The illustrated examples are plotted in Fig. 4, in which only the first three IMFs for SSE and the simulation data with $\beta = 0.8$ and their corresponding residuals are shown, the residual has been recognized as the trend of the given data.

According to the results of EMD theory, r_t is decomposed into 10 IMFs and each IMF is independent from the others. The term "independent" here is equivalent to the term "orthogonal" in the theory of finite dimensional vector space in some extent. That is, each IMF cannot be represented by other IMFs decomposed from the same primary time series [50]. Time

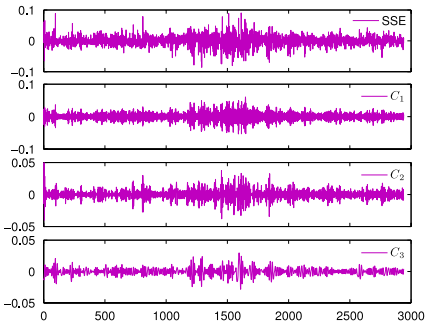

(a) SSE.

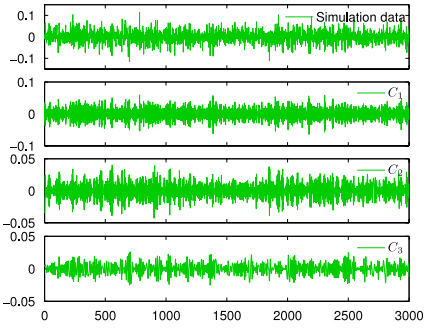

(b) Simulation data with $\beta = 0.8$.

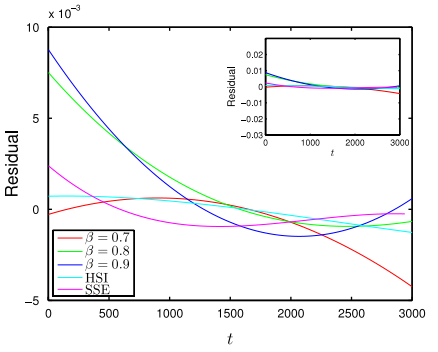

(c) Residuals for actual and simulation data series.

Fig. 4. (a) (b) The return series and the corresponding IMFs derived from EMD. (c) Residuals derived from EMD for actual and simulation data series, the inset is the mini form.

series will be decomposed by EMD method into several high and low frequency series, in an intuitive view, data is split into high volatility and lower volatility. In financial time series, high frequency data generally represents short-term trend meanwhile lower frequency exhibit the long-term volatility tendency. We aim to find some crucial difference or regularity between these IMFs.

As exhibited in Fig. 4, C_1 (defined in Fig. 2(a), the flowchart of EMD) seizes the main structures and characterizes the fastest fluctuations of the SSE and the same to the simulation data, because IMF C_1 is the first mode after the sifting process and it has the highest frequency among 10 IMFs. When we calculate the data with sifting process one more time, the frequency of the data will be lower than the former. As is shown in Fig. 4, both the simulated IMFs and the SSE IMFs have the similar frequency. In the residual map, the curves of $\beta = 0.8$ and $\beta = 0.9$ are reducing before they rise up while the situation is different when $\beta = 0.7$, even so, they have an overall declining trend. For comparison, the actual residuals is milder than the simulated residuals and their tendency is also decreasing, but to be precise, there is almost no distinction about the value between them, the inset picture could show us.

4.4. Analysis of absolute returns and absolute IMFs

Lacasa et al. [36] developed the visibility graph (VG) method, by which the investigation of a time series is performed through the mapping on networks or graphs. By means of such a mapping, the dynamical properties of time series are converted into the topological properties of networks, and, vice versa, the characteristics and features of time series can be inferred from those of networks. Compared to other methods which transform times series into complex networks, visibility graphs have a straight-forward geometric interpretation of the original time series, and are therefore suitable for quantitative analysis of the time series of financial market series. We apply the visibility algorithm to investigate the behaviors of absolute return time series and their corresponding absolute first three IMFs. (In the following, we use A.SSE, A.HSI, A.IMFs to represent these time series' absolute forms respectively.) In this analysis, to prove the rationality of the financial price model, the different statistical properties of the visibility graph and the horizontal visibility graph derived from the model and the actual data are comparatively studied by empirical research. Furthermore, we intend to compare the difference between the absolute forms of return series and IMFs series. In order to display a brief description of visibility graph, we plot the visibility graph mapped from A.SSE and its corresponding adjacent matrix in Fig. 5.

Fig. 5(b) gives a clear view about the intuitional difference between the two visibility algorithms. The adjacent matrix of VG has more approximal points than the HVG matrix graph, this may signify some statistical properties of VG algorithm are stronger than those of HVG algorithm because the adjacent matrix of VG embodies a tighter connection about the absolute

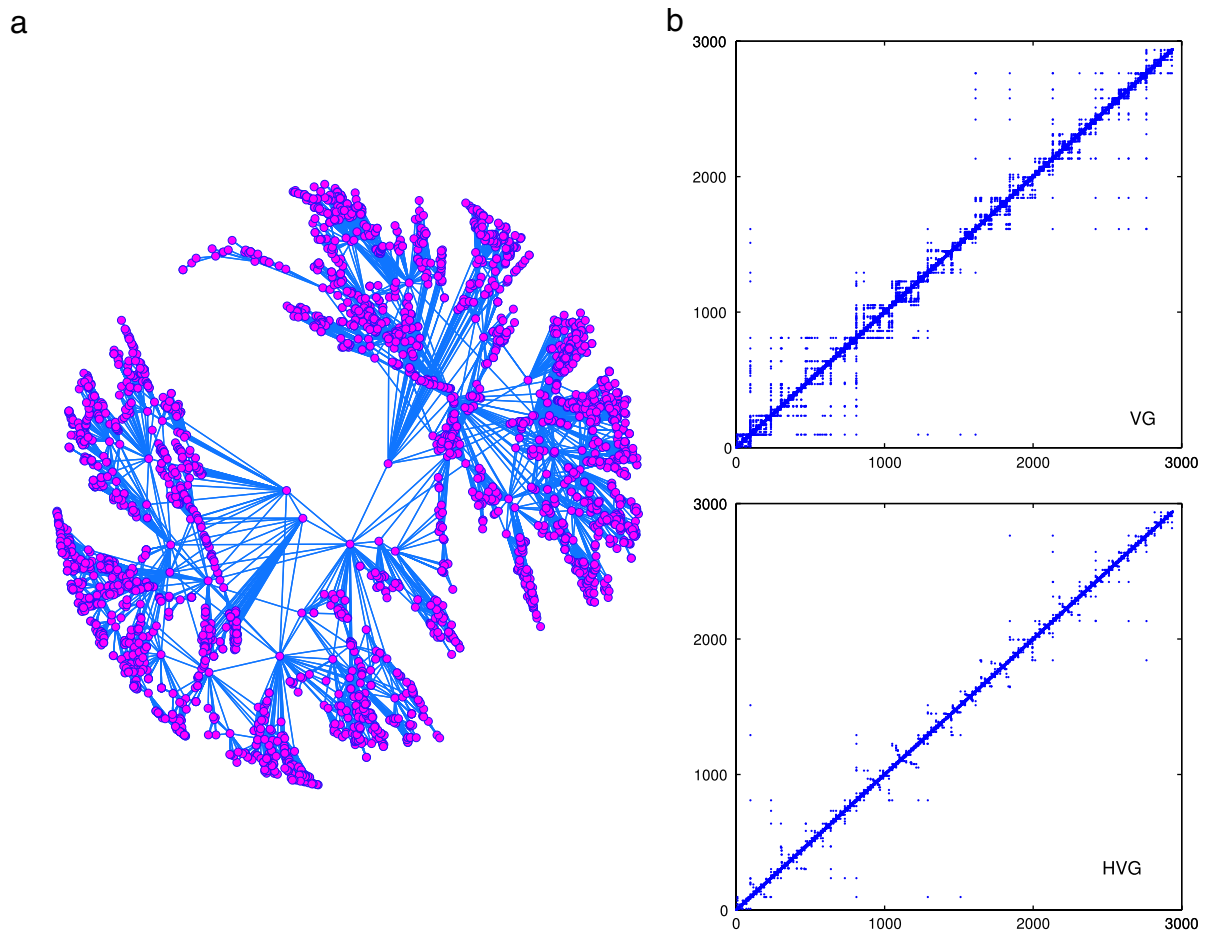

Fig. 5. Graphical illustrative examples derived from the absolute return series of the SSE. (a) Complex network graph mapped from visibility algorithm. (b) Top: the adjacent matrix of visibility algorithm; Bottom: the adjacent matrix calculated by horizontal visibility algorithm.

Table 3
Tail exponent α of degree distributions for VG.

α	A.simulation			SSE	HSI
	$\beta = 0.7$	$\beta = 0.8$	$\beta = 0.9$		
VG	3.152	2.989	3.046	2.929	2.541
HVG	5.212	5.331	5.406	5.223	5.484

return value. The complex network illustrative graph in Fig. 5(a) is drew based on the VG matrix, the vertex connection status is exhibited as plain as daylight. Among the network, there are some "key" vertices which themselves link with many other nodes and meanwhile these "key" points are connected to each other. The property is called "assortative" and will be studied later.

First of all, we focus on the degree distributions of vertices, Fig. 6 illustrates the cumulative distribution $P(k)$ of associate networks mapped form both the simulated and the actual absolute return series. Clearly, the VG graph and the HVG graph have the same trend and both comply with some kind of power law tail $P(k) \sim k^{-\alpha}$. Further, for a specific contrast, the estimated value of tail parameter α for visibility graph are figured out in Table 3. From Table 3, the exponent value of the absolute simulation data is vary close to the actual data's value, especially to the SSE. HVG's numerical value is larger than the VG's, it means that this kind of network translated by HVG logarithm exhibited a stronger power law tail than another logarithm. It illustrates that the financial model is reasonable to the real market in some extent, is more suitable for the SSE.

In order to further observe the behaviors of financial series and investigate whether the IMFs obtained from EMD method can also possess the basic network property as the original absolute return series, the cumulative degree distribution of the original series and their corresponding IMFs are exhibited in Fig. 7. For the three semi-log pictures, we can have a brief view about the relationship between return series and their IMFs. As the sifting process continued, the semi-log curves are higher than the original ones. Not only the A.SSE in Fig. 7(b), but also the simulation data in (a) and (c). Another point is, their

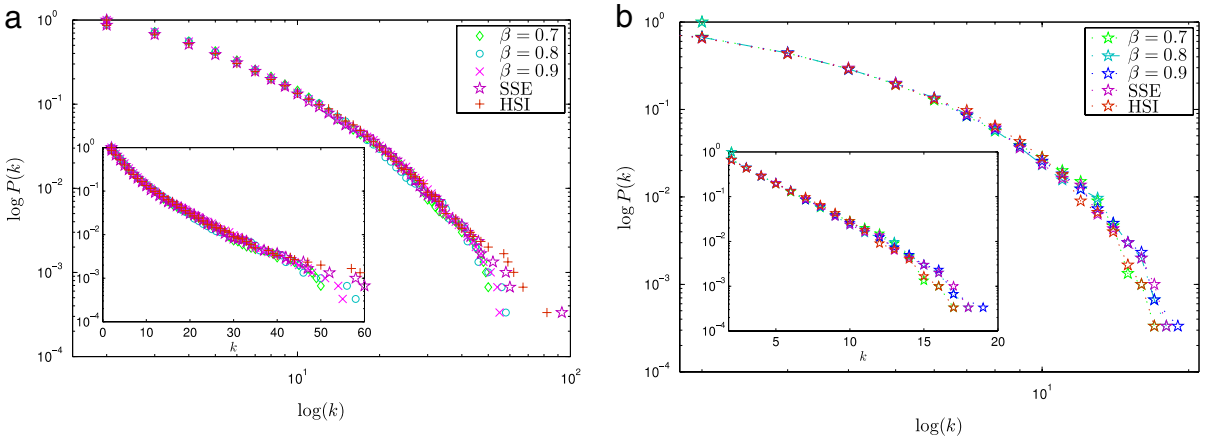

Fig. 6. Degree distributions of absolute simulation series, A.SSE and A.HSI: (a) VG, (b) HVG.

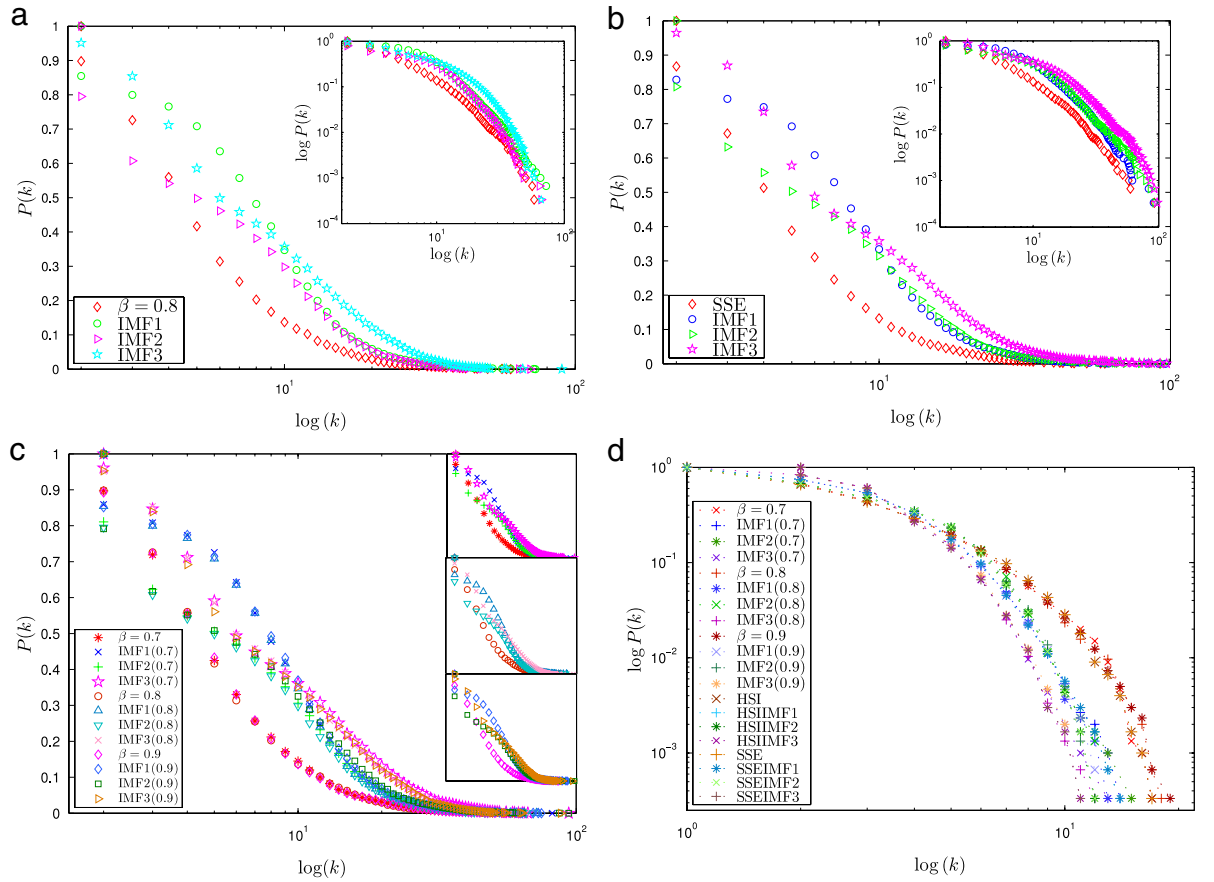

Fig. 7. Vertex degree distributions: (a) A.IMFs for the simulation data with $\beta = 0.8$; (b) A.IMFs for the SSE; (c) A.IMFs with three simulation series; (d) A.IMFs of the SSE, the HSI and the simulation data. ((a)–(c) are the semi-log plots of VG algorithm, and (d) is the log–log plot of HVG algorithm.)

equivalent log–log forms all have the power law behavior. Fig. 7(d) presents the HVG graph which contains three simulation series, two actual and their first three IMFs. Obviously, there is no much points as in VG graph, while the power law tail is conspicuous. The A.IMFs' curves is a bit deviated from the original series. And as the sifting process continued, the power law property is weaker than the former.

The assortative mixing pattern is also an important property for the complex network. To verify whether the simulation data and the actual data could present this character, the average degree $\langle k_n \rangle$ of the nearest neighbors of nodes for the simulation and the actual absolute return series are shown in Fig. 8. It is observable that as the degree k increases, the

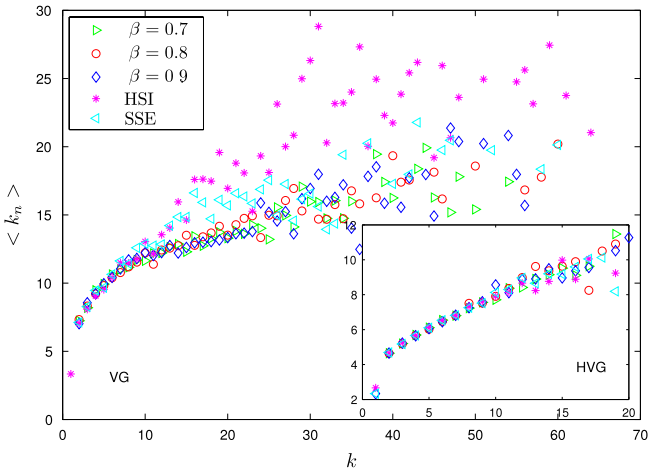

Fig. 8. Dependence of the average degree $\langle k_n \rangle$ of the nearest neighbors of nodes of the same degree k with respect to k for simulation and actual absolute return series. The inset: horizontal visibility graph algorithm.

Table 4
Pearson Coefficients for the simulation return series, the actual return series and the corresponding IMFs (absolute forms).

P.C.	VG				HVG			
	Original	IMF1	IMF2	IMF3	Original	IMF1	IMF2	IMF3
SSE	0.1561	0.2456	0.2579	0.3433	0.2933	0.2163	0.2725	0.4183
HSI	0.2791	0.1720	0.1921	0.2623	0.2928	0.2180	0.2735	0.4094
$\beta = 0.7$	0.1668	0.2459	0.3112	0.3652	0.2979	0.2292	0.2561	0.3911
$\beta = 0.8$	0.1802	0.2420	0.3096	0.3924	0.3072	0.2310	0.2788	0.4027
$\beta = 0.9$	0.1833	0.2629	0.2784	0.3743	0.3057	0.2348	0.2580	0.4097

Note: Pearson Coefficient is marked by P.C.

average degree $\langle k_n \rangle$ also does increase for both VG and HVG. In visibility graph, the most part of the SSE and HSI's curves are higher than that of the simulation ones, while in horizontal visibility graph all curves almost have the same trend and the same average degree. On one hand, the simulation return series and the actual financial return series are both provided with assortative mixing pattern, it is proved that high-degree vertices associate preferentially with other high-degree vertices in the financial model system. On the other hand, the degree correlation calculated through VG algorithm of the actual data has a stronger property than that of the simulation data, but the distinguish is not significant. This shows that the proposed series model is very close to the real market.

Assortative mixing pattern property is shown above. In other words, the property shows hubs are very likely to be linked together. A fact is revealed that the higher data height, the larger vertex degree [22]. And the price information is exhibited in absolute returns. Generally, the spreading of information will cause the fluctuations of stock price, further, the absolute returns will show fluctuations. So we speculate that assortative mixing represents there exists some kind of links between a strong financial information and another stronger information. The information may contain the investors' investment strategy, bad or good news, etc.

Then we detect the assortative property of the first three A.IMFs for the simulation data and two real indices, and give a concise comparison between A.IMFs and their originality. It is obviously seen from Fig. 9 that these five series and their corresponding IMFs all exhibit some assortative mixing pattern, and it seems like IMF3 series own the strongest assortative property. For giving a detail convince, the Pearson coefficients are calculated in Table 4. With an intuitive viewpoint, all quantitative values in Table 4 are positive, so we could have the conclusion that, from the acknowledge of Section 3.2, the network constructed by VG and HVG from all the real series, the simulation return series and the IMFs which we chose are assortative.

Furthermore, the data in Table 4 has some certain regularity. At first, in VG part, the value has an increasing tendency from originality to IMFs just exclusive of HSI, while in HVG part, the original data are all bigger than those of IMF1, the increasing tendency occurs from IMF1 to IMF3. As is known, the formation mechanism is different between the SSE and the HSI, so there is an inference visibility graph could distinguish different systems better than the horizontal visibility graph. On the second, the simulation data has the analogical value and very approximate trend to the SSE, particularly when $\beta = 0.7$ and $\beta = 0.8$.

5. Multiscale entropy analysis

Multiscale entropy (MSE) analysis has been applied to various types of data in physics and physiologic time series [41,42,63]. It is a method to measure the disorder and complexity of finite time series. Compared to traditional entropy,

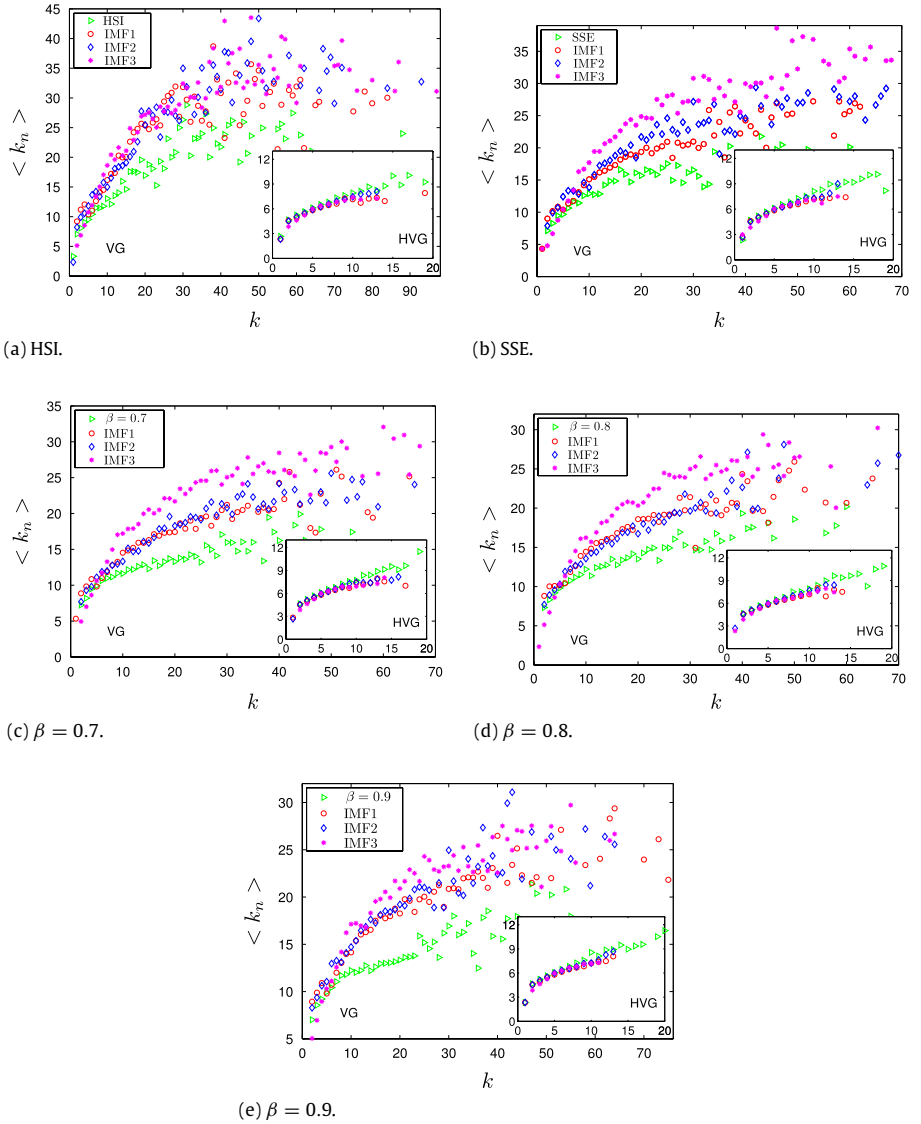

(a) HSI. (b) SSE.

(c) $\beta = 0.7$. (d) $\beta = 0.8$.

(e) $\beta = 0.9$.

Fig. 9. (a)–(e) Degree correlation relationships of absolute return series and the corresponding IMFs derived from EMD.

the multiscale entropy (MSE) approach measures the complexity of the system taking into account the multiple time scales. This computational tool can be quite effectively used to quantify the complexity of a given time series from many research areas, such as electroseismic time series [64], crude oil time series [65] and vibrations of a vehicle [66] and other field [67]. Costa et al. [41] used MSE to analyze the biological time series with succeeding in separating healthy and unhealthy groups. Multiscale entropy is based on the estimation of sample entropy (SampEn) which is a statistical measure proposed by Richman and Moorman [68]. In this section, we analyze the complexity of financial time series derived from real stock markets and the simulation data by MSE analysis, further, the complexity between IMFs and their original are also considered.

MSE method incorporates two significant procedures: (i) Coarse-graining process. Given a one-dimensional time series of N points $\{x_j : 1 \leq j \leq N\}$, multiscale coarse-grained time series are constructed by averaging the data points within non-overlapping windows of increasing length τ. Each point $y_j^{(\tau)}$ is defined as

$$y_j^{(\tau)} = \frac{1}{\tau} \sum_{i=(j-1)\tau+1}^{j\tau} x_j, \quad 1 \leq j \leq N/\tau \tag{10}$$

where τ represents the scale factor. For a given τ, the length of corresponding coarse-grained series is N/τ. So for scale one, the time series $y^{(1)}$ is simply the original series. (ii) SampEn process. The sample entropy S_E is calculated for each coarse-grained series, and then plotted as a function over the scale factor, for detail, see Refs. [44,41]. Then S_E is figured out. The

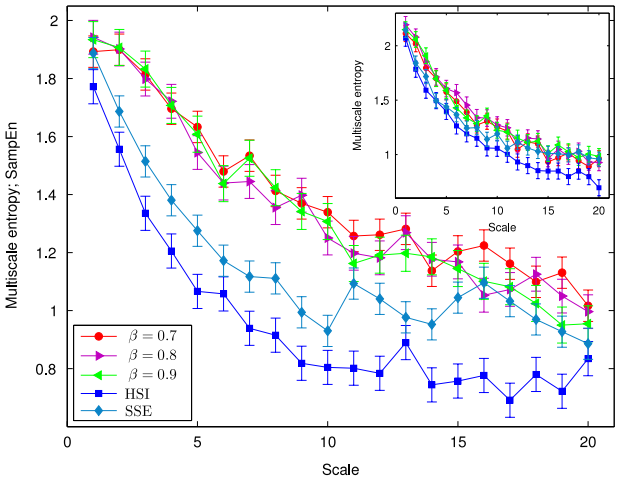

Fig. 10. MSE curves of absolute returns for the SSE, the HSI and the financial model with different values of β. The inset: original return series. Error bars: 20% standard error of the entropy series.

MSE curves are applied to compare the relative complexity of time series based on the following guidelines [42]: (a) if for the majority of the scales the SampEn values are higher for one time series than for another, the former is considered more complex than the latter; (b) a decrease of the entropy values indicates the original signal contains information only in the smallest scale.

Then the multiscale entropy for the SSE, the HSI and the financial model with different values of β is calculated and plotted in Fig. 10. From the figure we can see, the simulation series is considered more complex than that two indices for not only the absolute form but also the original return series. On the other side, the entropy curves of the simulation data are much closer to SSE's curve than HSI's. This is also an evidence to show that the financial model is more suitable for the SSE's system.

For digging out the complexity relationship for the original return series and their corresponding IMFs, the SampEn curves are plotted in Fig. 11(a)–(c) are the original return series and their first three IMFs for the SSE, the HSI and the simulation data with $\beta = 0.8$. They show that, the curve of original return series in each of the three pictures is higher than the other three IMFs curves, this means that IMFs series are less complex than the original one. Although IMF1 is the most similar to the original series, but it is less complex because of the lower frequency. When it occurs to IMF3, the trend is definitely changed, the curve increases before declining. For the absolute return series, the illustrated SampEn values have changed a lot. The multiscale entropy of IMFs in each picture become higher than their original series values and the curves are bouncing. Based on the MSE theory, the complexity of absolute IMFs are stronger than the absolute return series. We also can see, whether the original series or the absolute form, the situation for all the SSE, the HSI and the simulation data with $\beta = 0.8$ is almost the same. The simulation data derived from the proposed financial price model is reasonable to a large extent.

6. Conclusion

In the present paper, an agent-based stock price model is established by applying Ising system to investigate the volatility behavior of financial time series. We study the statistical properties of the financial model for different intensity values of β. And we comparatively study the properties of the simulation data with Shanghai Composite Index and Hang Seng Index. Through empirical mode decomposition analysis, the reduced frequency series IMFs are figured out, return series is decomposed into high volatility frequency and lower volatility frequency. Then we use visibility graph and horizontal visibility graph algorithms to translate the time series into assortative networks, and investigate the statistical properties of degree distribution and assortative mixing pattern further. The empirical research shows that the complex networks based on VG and HVG exhibit significant power law tail for the vertex degree distribution and evidently assortative mixing. In the network, high degree vertex is usually converted by one larger value, the assortative property is just said larger value prefers to link with another larger value. In other words, the property shows hubs are very likely to be linked together. And the price information is exhibited in absolute returns. Generally, the spreading of information will cause the fluctuations of stock price, further, the absolute returns will show fluctuations. So we speculate that assortative mixing represents there exists some kind of links between a strong financial information and another stronger information. The information may contain the investors' investment strategy, bad or good news, etc. Further, we use the multiscale entropy analysis to comprehend the complexity about the return series and their corresponding IMFs including the absolute form and original ones. The empirical results show that the complexities of the proposed model, the SSE and the HSI have the similar behaviors. To sum up, using the combined tools, we aim to analyze some specific properties of financial market series and simulation series produced

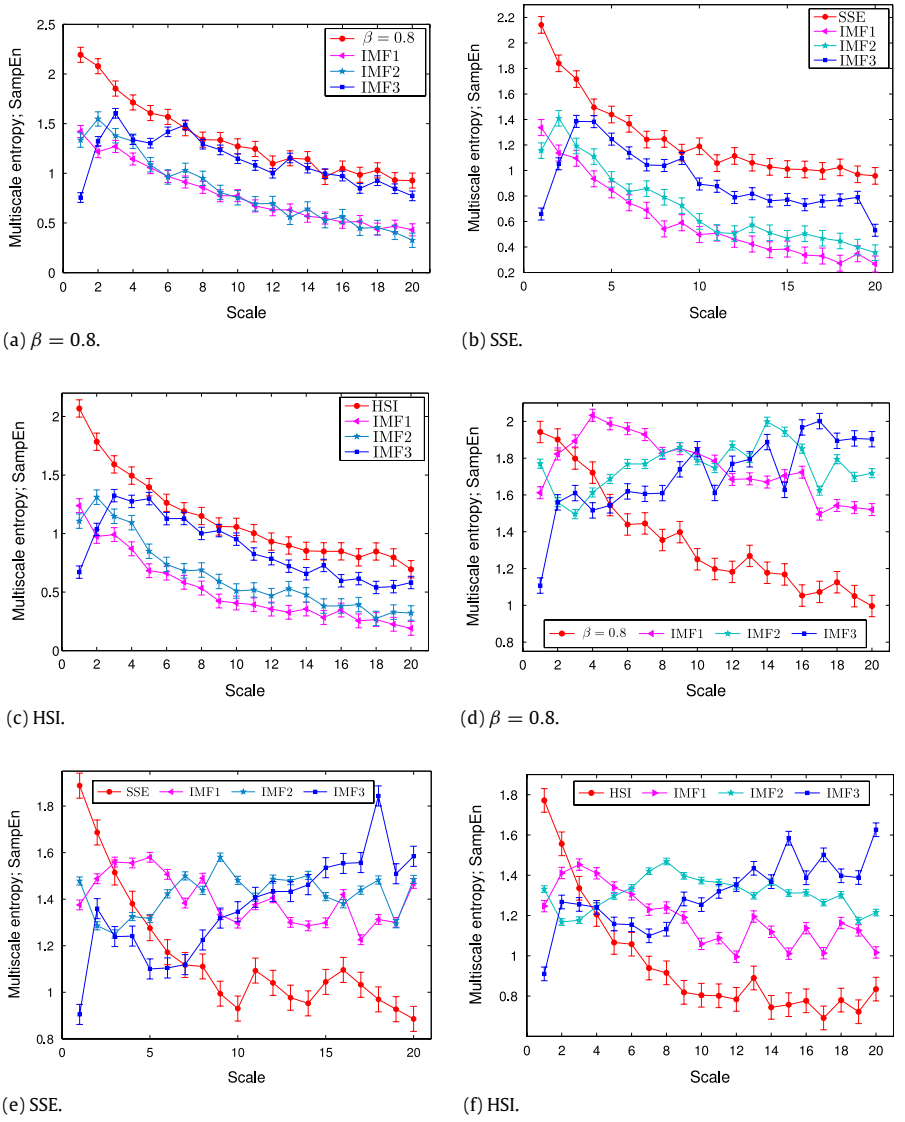

(a) $\beta = 0.8$. (b) SSE.

(c) HSI. (d) $\beta = 0.8$.

(e) SSE. (f) HSI.

Fig. 11. Multiscale entropy analysis for the SSE, the HSI and the simulation series with $\beta = 0.8$ and their corresponding IMFs. (a)–(c) Original return series; (d)–(f) Absolute return series. Error bars: 20% standard error of the entropy series.

by Ising interacting system, in order to demonstrate the effectiveness of our model from multiple perspectives. Through the comparisons between the real markets and the simulation data, we hope to show that the financial model of the present paper is reasonable to some extent. For another thing, we hope to dig out some internal volatility regularity generated by different frequency by means of the empirical mode decomposition method. What is more, the volatility behavior is gradually changing after we translate time series into assortative networks. That means frequency plays a significant role in volatility behavior, especially exhibits large distinction in complexity analysis.

Acknowledgment

The authors were supported in part by National Natural Science Foundation of China Grant Nos. 71271026 and 10971010.

References

[1] F. Black, M. Scholes, The pricing of options and corporate liabilities, J. Polit. Econ. 81 (1973) 637–654.
[2] J.P. Bouchaud, M. Potters, Theory of Financial Risk and Derivative Pricing: From Statistical Physics to Risk Management, Cambridge University Press, Cambridge, 2003.
[3] W.Y. Cheng, J. Wang, Dependence phenomenon analysis of the stock market, Europhys. Lett. 102 (2013) 18004.
[4] W. Fang, J. Wang, Statistical properties and multifractal behaviors of market returns by Ising dynamic system, Internat. J. Modern Phys. C 23 (2012) 1250023. 14 pages.

[5] W. Fang, J. Wang, Fluctuation behaviors of financial time series by a stochastic Ising system on a Sierpinski carpet lattice, Physica A 392 (2013) 4055–4063.
[6] W. Fang, J. Wang, Effect of boundary conditions on stochastic Ising-like financial market price model, Bound. Value Probl. 2012 (2012) 9.
[7] X. Gabaix, P. Gopikrishanan, V. Plerou, H.E. Stanley, A theory of power-law distributions in financial market fluctuations, Nature 423 (2003) 267–270.
[8] R. Gaylord, P. Wellin, Computer Simulations with Mathematica: Explorations in the Physical, Biological and Social Science, Springer-Verlag, New York, 1995.
[9] K. Ilinski, Physics of Finance: Gauge Modelling in Non-Equilibrium Pricing, Wiley, New York, 2001.
[10] A. Krawiecki, Microscopic spin model for the stock market with attractor bubbling and heterogeneous agents, Internat. J. Modern Phys. C 16 (2005) 549–559.
[11] D. Stauffer, T.J.P. Penna, Crossover in the Cont–Bouchaud percolation model for market fluctuations, Physica A 256 (1998) 284–290.
[12] D. Lamberton, B. Lapeyre, Introduction to Stochastic Calculus Applied to Finance, CRC Press, Boca Raton, 2007.
[13] Z. Liao, J. Wang, Forecasting model of global stock index by stochastic time effective neural network, Expert Syst. Appl. 37 (2010) 834–841.
[14] T. Lux, M. Marchesi, Scaling and criticality in a stochastic multi-agent model of a financial market, Nature 397 (1999) 498–500.
[15] T. Lux, Financial Power Laws: Empirical Evidence, Models and Mechanisms, Cambridge University Press, Cambridge, 2008.
[16] R.N. Mantegna, H.E. Stanley, Introduction to Econophysics: Correlations and Complexity in Finance, Cambridge University Press, Cambridge, 2000.
[17] T.C. Mills, The Econometric Modeling of Financial Time Series, second ed., Cambridge University Press, Cambridge, 1999.
[18] L. Feng, B. Li, B. Podobnik, T. Preis, H.E. Stanley, Linking agent-based models and stochastic models of financial markets, Proc. Natl. Acad. Sci. 109 (2012) 8388–8393.
[19] H.L. Niu, J. Wang, Volatility clustering and long memory of financial time series and financial price model, Digit. Signal Process. 23 (2013) 489–498.
[20] J. Wang, Q.Y. Wang, J.G. Shao, Fluctuations of stock price model by statistical physics systems, Math. Comput. Modelling 51 (2010) 431–440.
[21] T.S. Wang, J. Wang, J.H. Zhang, W. Fang, Voter interacting systems applied to Chinese stock markets, Math. Comput. Simul. 81 (2011) 2492–2506.
[22] D. Xiao, J. Wang, Graph based and multifractal analysis of financial time series model by continuum percolation, Int. J. Nonlinear Sci. Numer. 15 (2014) 265–277.
[23] Y. Yu, J. Wang, Lattice-oriented percolation system applied to volatility behavior of stock market, J. Appl. Stat. 39 (2012) 785–797.
[24] J.H. Zhang, J. Wang, Modeling and simulation of the market fluctuations by the finite range contact systems, Simul. Modell. Pract. Theory 18 (2010) 910–925.
[25] J.H. Zhang, J. Wang, J.G. Shao, Finite-range contact process on the market return intervals distributions, Adv. Complex Syst. 13 (2010) 643–657.
[26] W.J. Hong, J. Wang, Multiscale behavior of financial time series model from Potts dynamic system, Nonlinear Dynam. 78 (2014) 1065–1077.
[27] P.W. Anderson, More is different, Science 177 (1972) 393–396.
[28] F. Corsi, S. Mittnik, C. Pigorsch, U. Prgorsch, The volatility of realized volatility, Econometric Rev. 27 (2008) 46–78.
[29] P. Grau-Carles, Long-range power-law correlations in stock returns, Physica A 299 (2001) 521–527.
[30] A.W. Lo, Long-term memory in stock market price, Econometrica 59 (1991) 1279–1314.
[31] R.F. Engle, Autoregressive conditional heteroskedasticity with estimates of UK inflation, Econometrica 50 (1982) 987–1008.
[32] T. Bollerslev, Generalized autoregressive conditional heteroskedasticity, J. Econometrics 31 (1986) 307–327.
[33] A. Babikir, R. Gupta, C. Mwabutwa, E. Owusu-Sekyere, Structural breaks and GARCH models of stock return volatility: The case of South Africa, Ecol. Modell. 29 (2012) 2435–2443.
[34] S.R. Bentes, A comparative analysis of the predictive power of implied volatility indices and GARCH forecasted volatility, Physica A 424 (2015) 105–112.
[35] V. Plerou, B. Rosenow, L.A.N. Amaral, H.E. Stanley, Econophysics: financial time series from a statistical physics point of view, Physica A 279 (2000) 443–456.
[36] L. Lacasa, B. Luque, F. Ballesteros, J. Luque, J.C. Nuno, From time series to complex networks: the visibility graph, Proc. Natl. Acad. Sci. 105 (2008) 4972–4975.
[37] L. Lacasa, B. Luque, J. Luque, J.C. Nu, The visibility graph: a new method for estimating the Hurst exponent of fractional Brownian motion, Europhys. Lett. 86 (2009) 30001.
[38] B. Luque, L. Lacasa, F. Ballesteros, J. Luque, Horizontal visibility graphs: exact results for random time series, Phys. Rev. E 80 (2009) 046103.
[39] N.E. Huang, S. Zheng, S.R. Long, M.C. Wu, H.H. Shih, Q. Zheng, N.C. Yen, C.C. Tung, H.H. Liu, The empirical mode decomposition and the Hilbert spectrum for nonlinear and nonstationary time series ayalysis, Proc. R. Soc. Lond. Ser. A 454 (1998) 903–995.
[40] N.E. Huang, M.C. Wu, S.R. Long, S.S.P. Shen, W. Qu, P. Gloersen, K.L. Fan, A confidence limit for the empirical mode decomposition and Hilbert spectral analysis, Proc. R. Soc. Lond. Ser. A 459 (2003) 2317–2345.
[41] M. Costa, A.L. Goldberger, C.K. Peng, Multiscale entropy analysis of complex physiological time series, Phys. Rev. Lett. 89 (2002) 4. Article ID 068102.
[42] M. Costa, C.K. Peng, A.L. Goldberger, J.M. Hausdoff, Multiscale entropy analysis of human gait dynamics, Physica A 330 (2003) 53–60.
[43] M.F. Chen, From Markov Chains to Non-Equilibrium Particle Systems, second ed., World Scientific, River Edge, NJ, USA, 2004.
[44] R.S. Ellis, Entropy, Large Deviations, and Statistical Mechanics, Springer-Verlag, New York, 1985.
[45] T.M. Liggett, Interacting Particle Systems, Springer-Verlag, New York, 1985.
[46] T.M. Liggett, Stochastic Interacting Systems: Contact, Voter and Exclusion Processes, Springer-Verlag, Berlin, Heidelberg, 1999.
[47] F. Wang, J. Wang, Statistical analysis and forecasting of return interval for SSE and model by lattice percolation system and neural network, Comput. Ind. Eng. 62 (2012) 198–205.
[48] J. Wang, The estimates of correlations in two-dimensional Ising model, Physica A 388 (2009) 565–573.
[49] S.M. Ross, An Introduction to Mathematical Finance, Cambridge University Press, Cambridge, 1999.
[50] H.L. Niu, J. Wang, Phase and multifractality analyses of random price time series by finite-range interacting biased voter system, Comput. Statist. 29 (2014) 1045–1063.
[51] X.Y. Qian, G.F. Gu, W.X. Zhou, Modified detrended fluctuation analysis based on empirical mode decomposition for the characterization of anti-persistent processes, Physica A 390 (2011) 4388–4395.
[52] J. Zhang, M. Small, Complex network from pseudo periodic time series: topology versus dynamics, Phys. Rev. Lett. 96 (2006) 238701.
[53] X. Xu, J. Zhang, M. Small, Superfamily phenomena and motifs of networks induced from time series, Proc. Natl. Acad. Sci. USA 105 (2008) 19601–19605.
[54] J.O. Pierini, M. Lovallo, L. Telesca, Visibility graph analysis of wind speed records measured in central Argentina, Physica A 391 (2012) 5041–5048.
[55] L. Telesca, M. Lovallo, Analysis of seismic sequences by using the method of visibility graph, Europhys. Lett. 97 (2012) 50002.
[56] L. Telesca, M. Lovallo, A. Ramirez-Rojas, L. Flores-Marquez, Investigating the time dynamics of seismicity by using the visibility graph approach: application to seismicity of Mexican subduction zone, Physica A 392 (2013) 6571–6577.
[57] L. Telesca, M. Lovallo, J.O. Pierini, Visibility graph approach to the analysis of ocean tidal records, Chaos Solitons Fractals 45 (2012) 1086–1091.
[58] X. Tang, L. Xia, Y. Liao, W. Liu, Y. Peng, T. Gao, Y. Zeng, Newapproach to epileptic diagnosis using visibility graph ofhigh-frequency signal, Clin. EEG Neurosci. 44 (2013) 150–156.
[59] G. Zhu, Y. Li, P. Wen, Epileptic seizure detection in EEGs signals using a fast weighted horizontal visibility algorithm, Comput. Methods Programs Biomed. 115 (2014) 64–75.
[60] M.E.J. Newman, The structure and function of complex networks, SIAM Rev. 45 (2003) 167–256.
[61] M.E.J. Newman, Assortative mixing in networks, Phys. Rev. Lett. 89 (2002) 208701.
[62] M.E.J. Newman, Mixing patterns in networks, Phys. Rev. E 67 (2003) 026126.
[63] R.A. Thuraisingham, G.A. Gottwald, On multiscale entropy analysis for physiological data, Physica A 366 (2006) 323–332.
[64] L.G. Vargas, A.R. Rojas, F.A. Brown, Multiscale entropy analysis of electroseismic time series, Nat. Hazards Earth Syst. Sci. 8 (2008) 855–860.
[65] E. Martina, E. Rodriguez, R.E. Perez, J.A. Ramirez, Multiscale entropy analysis of crude oil price dynamics, Energy Econ. 33 (2011) 936–947.
[66] G. Litak, A. Syta, R. Rusinek, Dynamical changes during composite milling: recurrence and multiscale entropy analysis, Int. J. Adv. Manuf. Technol. 56 (2011) 445–453.
[67] H.L. Niu, J. Wang, Quantifying complexity of financial short-term time series by composite multiscale entropy measure, Commun. Nonlinear Sci. Numer. Simul. 22 (2015) 375–382.
[68] J.S. Richman, J.R. Moorman, Physiological time-series analysis using approximate entropy and sample entropy, Am. J. Physiol. Heart Circ. 278 (2000) H2039–H2049.